

Hologram: Realtime Holographic Overlays via LiDAR Augmented Reconstruction

Ekansh Agrawal

UC Berkeley EECS

USA

agrawalekansh@berkeley.edu

ABSTRACT

Guided by the hologram technology of the infamous Star Wars franchise, I present an application that creates real-time holographic overlays using LiDAR augmented 3D reconstruction. Prior attempts involve SLAM or NeRFs which either require highly calibrated scenes, incur steep computation costs, or fail to render dynamic scenes. I propose 3 high-fidelity reconstruction tools that can run on a portable device, such as a iPhone 14 Pro, which can allow for metric accurate facial reconstructions. My systems enable interactive and immersive holographic experiences that can be used for a wide range of applications, including augmented reality, telepresence, and entertainment.

CCS CONCEPTS

• **Computing methodologies** → **Structured outputs; Neural networks; Volumetric models.**

KEYWORDS

Computer vision, LiDAR, SLAM, 3D reconstruction, Deep learning

ACM Reference Format:

Ekansh Agrawal. 2024. Hologram: Realtime Holographic Overlays via LiDAR Augmented Reconstruction. In *Proceedings of UC Berkeley EECS (COMPSCI 280 '24)*. ACM, New York, NY, USA, 8 pages. <https://doi.org/XXXXXXX.XXXXXX>

1 MOTIVATION

As a kid, an engineer, and a researcher, the world of Stars Wars has never stopped to pique my curiosity. Whether it's the fast-than-light intergalactic space travel or the iconic laser sword "lightsabers", the Star Wars universe has always been a source of inspiration for me. One of the most iconic technologies in the Star Wars universe is the hologram as shown in. Soldiers, politicians, and civilians alike all use portable devices to project 3D images of people or objects in real-time to communicate in real-time. This technology has been a staple in the Star Wars franchise and in this project, I aim to bring this technology to life. My goal is to create a system that can project real-time holographic overlays using LiDAR augmented 3D reconstruction. The idea of a hologram is not just a cool visual effect,

Permission to make digital or hard copies of all or part of this work for personal or classroom use is granted without fee provided that copies are not made or distributed for profit or commercial advantage and that copies bear this notice and the full citation on the first page. Copyrights for components of this work owned by others than the author(s) must be honored. Abstracting with credit is permitted. To copy otherwise, or republish, to post on servers or to redistribute to lists, requires prior specific permission and/or a fee. Request permissions from permissions@acm.org.

COMPSCI 280 '24, May '24, Berkeley, CA

© 2024 Copyright held by the owner/author(s). Publication rights licensed to ACM.

ACM ISBN 978-1-4503-XXXX-X/24/04

<https://doi.org/XXXXXXX.XXXXXX>



Figure 1: Hologram technology from the Star Wars universe

but a powerful tool that can be used for a wide range of applications, including augmented reality, telepresence, and entertainment.

While there have been many notable hardware advancements in 3D reconstructions and holographic displays, there are still many challenges that need to be addressed before they can be proposed as an everyday consumer electronic [29] [30] [41] [53]. For the scope of this project, I focus solely on software as a vehicle of real-time reconstructions. I also further narrow the scope by mostly focusing on trying to reconstruct faces. Existing methods rely on highly calibrated environments, incur steep computation costs, or fail to render dynamic scenes [67]. In this project, I propose three high-fidelity reconstruction tools that can run on a portable device, such as an iPhone 14 Pro, which can allow for metric accurate facial reconstructions. These systems enable interactive and immersive holographic experiences that can be used for a wide range of applications, including augmented reality, telepresence, and entertainment.

2 PRIOR WORKS

2.1 Simultaneous Localization and Mapping

With the introduction of the Kinect Sensor, low-resolution depth and visual sensing introduced novel approaches for real-time real-time dense 3D reconstruction [13]. Initial research employs a volumetric truncated signed distance function (TSDF) to fuse depth data into a global model. KinectFusion achieves impressive results but is limited to relatively small-scale environments due to memory constraints [17]. ElasticFusion extends KinectFusion by introducing a more flexible and scalable map representation using surfels (surface elements) [63]. It can handle larger environments and loop closures, enabling robust and consistent reconstructions. Real-time 3D reconstruction system that combines depth and RGB data. It

leverages the complementary strengths of geometric and photometric information, resulting in high-quality reconstructions with accurate geometry and detailed texture [9]. Research has allowed large-scale, real-time 3D reconstructions via multiple Kinect sensors by efficiently allocating and updating only the occupied regions in the volume [36] [51] [43].

While these methods have made significant progress in real-time 3D reconstruction, they are limited to static environments and struggle to handle dynamic scenes in high resolution. This makes live reconstruction of a high detail object like a subject's face temperamental. They rely on geometric priors and are sensitive to noise and outliers in the input data. Furthermore, most of these methods rely on the Kinect Sensor which is not as portable as the project goal.

2.2 Depth Estimation

Depth estimation of a scene allows us to perform classical image transformations to scale coordinates from the image plane to the world plane. This is a crucial step in 3D reconstruction as it allows us to map the 2D image to a 3D point cloud quite effortlessly given the frame depth and calibration parameters. Traditional methods for depth estimation include stereo matching, structure from motion, and depth from de-focus. Stereo matching involves finding correspondences between two images taken from different view-points and computing a disparity map of some kind [50] [4]. This techniques usually are contingent on a highly calibrated environment in order to use epipolar geometry to extrapolate between the 3D points and their projections onto the 2D images [23] [33]. More recent advances in stereo vision include the use of CNNs for disparity estimation [68] [22]. Significant progress has also been made in the realm of monocular depth estimation via deep learning approaches that learn to extract relevant features and depth cues from large-scale datasets of RGB images and corresponding depth maps [11] [26]. Advancements like encoder-decoder architectures [24] [15], attention mechanisms and multi-task learning [7] [62], transformers-based architectures [45] [8], and even diffusion-based architecture [49] [21] have all attempted to reduce the disparity of a neural based approach for depth estimation.

Structure from motion techniques aim to reconstruct 3D structures from a sequence of 2D images captured from different view-points. Basic techniques involve extrapolating an essential matrix between the images and then using the epipolar geometry to triangulate the 3D points [28] [59] [42]. More recent advances in structure from motion include the use of deep learning techniques to estimate the camera poses and 3D points [61] [70]. My major qualm with adopting these techniques is the need for a highly calibrated environment. These techniques also rely heavily on using more than one camera to capture the scene [69]. I introduce engineering constraints later in this project which make it difficult to adopt this approach.

3D reconstructions via LiDAR involve processing and interpreting these point cloud data to create accurate 3D models or representations of objects, scenes, or environments. Through time-of-flight calculations, LiDAR technology can create efficient point cloud registration [3] [65] which can be used for surface reconstruction [20] [38]. Deep learning approaches [16] [18] are instrumental for

large-scale scene reconstruction [39] [37]. The main problem with consumer grade LiDAR sensors are their lack of precision [32], and industrial grade sensors can cost tens of thousands of dollars making their usage cost prohibitive [64].

2.3 Neural Radiance Fields

The advent of NeRFs introduced an approach to synthesizing novel views [34], highlighting their abilities to capture and render complex scenes with high fidelity [35] [58], including intricate geometric details, view-dependent effects (e.g., specular, transparency), and challenging lighting conditions [60] [66]. This is achieved by the high-dimensional and continuous nature of the learned representation, which can encode rich scene properties without relying on explicit 3D geometry or texture mapping [34]. NeRFs have been extended to handle dynamic scenes by incorporating temporal information [25] [44], enabling the reconstruction of moving objects and scenes. Further optimizations introduced high quality renders with sparse input views [12] [27] and close to real-time rendering speeds for individual scenes [14] [47] [56] [57]. However, in order to achieve high-fidelity facial reconstructions, NeRFs require a large number of input views and high-resolution images, which can be computationally expensive and time-consuming. This makes it difficult to achieve real-time performance on portable devices, like the iPhone 14 Pro, since I would need to render a new scene for every frame.

3 METHODOLOGY

I propose three approaches to generating real-time 3D facial reconstructions in this paper. While these individual techniques may not be novel in nature, the hybrid approach along with the constraint of the real-time reconstruction requires quite a bit of engineering to get them to work with high fidelity. I self-imposed the following engineering constraints on my methodology to ensure that the engineered solutions were novel and challenging to implement:

- (1) **Monocular estimation:** Reconstruction cannot be performed with more than a single set of sensors. (IE. only one camera, one LiDAR sensor, etc..)
- (2) **Portability:** If the clone troopers carried around tiny portable devices, I want to be able to do same. No backup RTX 4090s.
- (3) **High fidelity:** The final rendered voxel grid cannot be insanely sparse. It should be extremely clear what's being rendered, and we should be able to tell exactly who's face is being reconstructed.
- (4) **Instantaneous:** A viable solution must achieve at least 30 FPS during reconstruction and must occur online.

3.1 Attempt 1: Monocular Depth Estimation

My initial approach, as shown in Figure 2, is quite simple in nature. Given an image frame, I want to use our classical projection formulas in order to transform image from the uv coordinate system to the world coordinate system. Calibrated environments can utilize stereo imaging to leverage disparity maps to compute depth over a calibrated scene. I can replace this depth approach with a monocular-depth estimation model. I use Intel MiDaS as the core backbone of my depth estimation pipeline, consisting of a ViT backbone pre-trained off of ImageNet [46] [5]. A single frame is passed

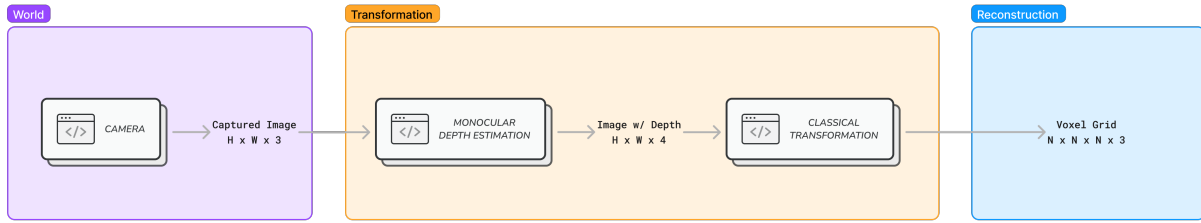


Figure 2: Attempt 1 utilizes monocular depth estimation alongside classical image projections in order to transfer pixels from their image representation into there voxel representation.

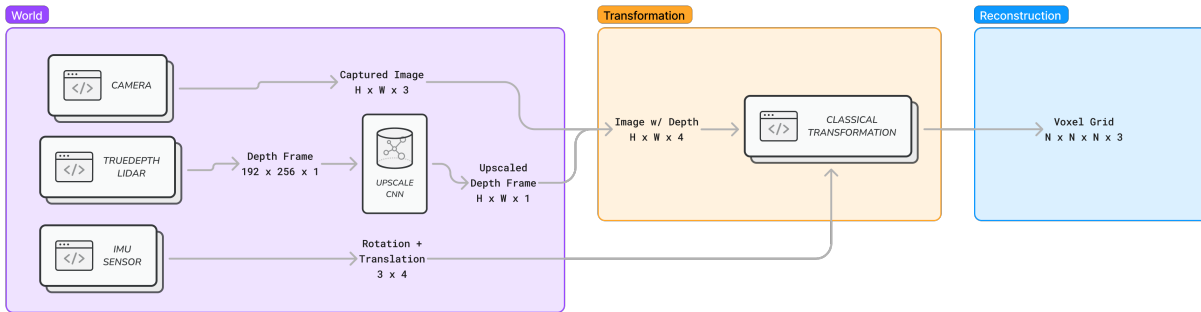


Figure 3: Attempt 2 utilizes the LiDAR and TrueDepth data streamed from the iPhone 14 Pro’s front facing sensors. This data is then upscaled with a SRCNN model trained on facial depth maps. I fuse this data and then use classical projections using the phone’s IMU sensor for camera poses.

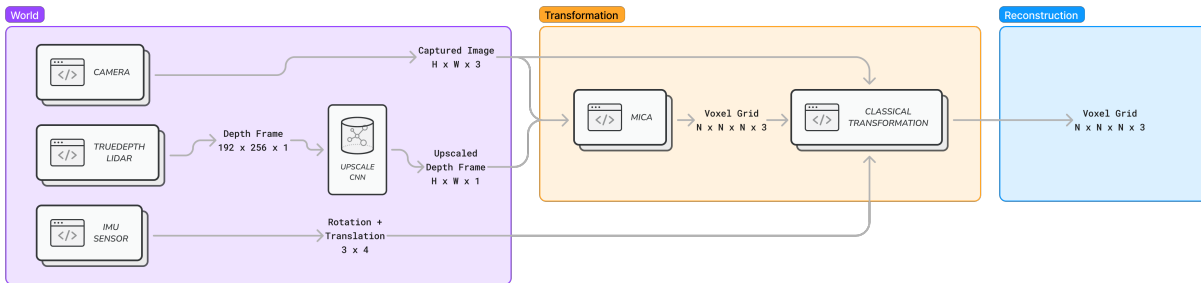


Figure 4: Attempt 3

into this model, and the output is a H by W matrix consisting of the relative depth of each pixel from the input image frame as z_c . I then extract the camera intrinsics from the webcam and apply Equation 1 to extract the camera points. I use identify transformations and apply Equation 2 to project the points into the world coordinate system.

$$\begin{bmatrix} x_c \\ y_c \\ z_c \end{bmatrix} = \begin{bmatrix} f_x & 0 & c_x \\ 0 & f_y & c_y \\ 0 & 0 & 1 \end{bmatrix} \begin{bmatrix} u \\ v \\ 1 \end{bmatrix} + \begin{bmatrix} 0 \\ 0 \\ z_c - 1 \end{bmatrix} \quad (1)$$

$$\begin{bmatrix} x_w \\ y_w \\ z_w \end{bmatrix} = R \begin{bmatrix} x_c \\ y_c \\ z_c \end{bmatrix} + T \quad (2)$$

As a means of comparison, I also used the Marigold diffusion model for depth estimation which utilizes a fine-tuned Stable Diffusion model [21]. I used 10 denoising steps and preserved the image resolution during model inferences.

3.2 Attempt 2: LiDAR + TrueDepth

The release of Apple’s iPhone 12 Pro introduced a consumer-grade LiDAR sensor and TrueDepth infrared depth sensor. The combination of these sensors project points onto the subject and record the time it takes for points to reflect light back into the sensors [31]. The LiDAR sensor works well with coarse objects while the TrueDepth sensors works well with differentiating distance between fine objects as shown in Figure 5.

For the second attempt, as shown in Figure 3, I replace the monocular depth estimation stack with the LiDAR sensor stack, using an

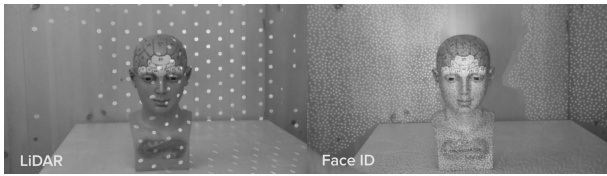


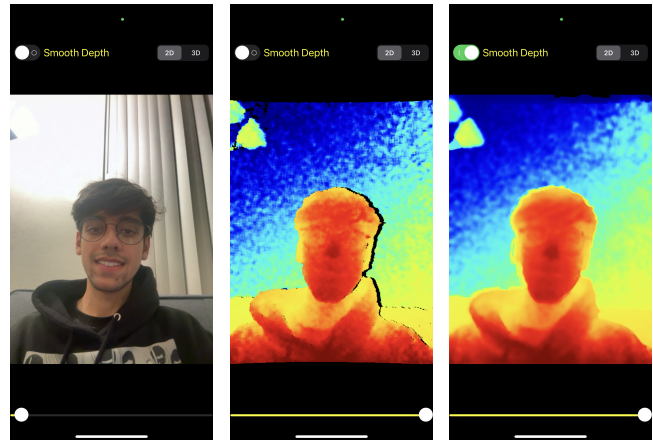
Figure 5: Projected light coordinates for the TrueDepth and LiDAR sensors shipped with the Apple iPhones.

iPhone 14 Pro as my test device. This required a rewrite in Swift in order to leverage the native Apple SDKs for GPU and LiDAR programming. Due to the low resolution of the LiDAR sensor, a custom trained SRCNN model was employed to upscale the LiDAR depth frame. This model was initially pre-trained on the Set5 super-resolution dataset [10] and then fine-tuned on a custom dataset of 10,000 face depth images. This dataset was constructed by using the Generated Photos Academic Dataset and feeding it through Marigold with 15 denoising steps for a depth frame. These images were then down scaled by a factor of 4 and anti-aliased for their lower resolution representations. The trained model was deployed via CoreML in order to leverage the Apple Neural Engine on the iPhone [1]. The results of SRCNN deployed to the LiDAR collection stack is shown in Figure 6. Figure 6b shows the depth results after a 4x upscale via basic bilinear interpolation. The occluded edges are more dramatic and the overall texture around the edges is more noisy. Figure 6c shows the depth results after a forward-inference through the SRCNN model, which shows a more consistent and higher fidelity depth rendering with a 4x upscaler. These screenshots were collected via my Swift application.

After passing the LiDAR data through the model and fusing it with the TrueDepth sensor data via weighted averaging, I used the classical transformation equations from above in order to project the voxels into their world coordinate representations. However, this time, instead of ignoring the extrinsic transformations, I was able to use the IMU sensor on the iPhone to extract the camera rotation and translation for the final transformations. I used Metal shaders to render the reconstructed voxel map in real-time via Apple’s GPU in my app.

3.3 Attempt 3: Template Modeling

The final attempt, as shown in Figure 4, was to leverage a deep-learning approach to render a facial reconstruction and apply texture + mesh transformations directly through an end-to-end approach. The intuition behind this approach was that a deep learning method would enable us to learn the general shape of a face and apply internal transformations to render real-time facial reconstructions given a webcam stream. This would potentially allow for more dynamic and responsive interactions in virtual environments, as the system could adjust and adapt to the user’s facial expressions and movements in real time. The initial goal was to use INSTA for volumetric avatar rendering given a single RGB frame, however the inference time was too slow for real-time rendering [71]. I instead used MICA, which tracks facial landmarks on a face, and then renders a 3D mesh that skews the landmarks from a global mean [72]. I modified this model slightly to use the fused and upscaled



(a) Raw image frame (b) LiDAR + True Depth fused frame upscaled with bilinear interpolation (c) LiDAR + True Depth fused frame upscaled with SR-CNN model

Figure 6: Lidar + TrueDepth data from iPhone 14 Pro generated from reconstruction app programmed in Swift + Metal

LiDAR + TrueDepth sensor data from the prior attempt to aid the model with more accurate metric reconstructions. I retrained MICA on the original dataset, which were a combination of images from LYHM [40], and FaceWarehouse [6], but fused a depth dimension generated via Marigold with 10 de-noising steps.

For real-time rendering, I pass the RGB image frame along with the pixel-wise depth frame through my modified version of MICA. This inference produces a mesh that I rasterize to receive its voxelized representation. Using the depth frame as a heuristic, I project pixels in the background into the rendered scene. Once again using the iPhone’s IMU sensor to extrapolate camera rotation and translation to apply final transformation to the rendered voxel grid. As noted in the Results sections, this approach wasn’t fully deployed on the iPhone due to some technical issues. Therefore, I was unable to fully render the scene which this approach and was limited to reconstructing the face.

4 RESULTS

4.1 Attempt 1: Monocular Depth Estimation

With the monocular depth estimation approach, reconstruction averaged around ~2 FPS with MiDAS and ~0.25 FPS when using Marigold on 10 de-noising steps. The other backbones available on Torch Hub resulted in the same fidelity reconstruction but larger model size, so I defaulted to using the default ViT backbone for my tests. These models were deployed to an iPhone using the PyTorch to CoreML pipeline for quantization and scheduling. An open-source CoreML diffusion model loader application was monkey patched to run inference on these deployed models on an iPhone 14 Pro. For Marigold, decreasing the number of steps introduced quite a few artifacts, and increasing the steps after 15 denoising steps didn’t seem to affect the reconstruction quite a lot. Figure 7 shows these reconstructions, with the 2nd and 4th row showcasing results



Figure 7: Reconstruction via monocular depth estimation with different model backbones. In this figure we show MiDaS with low fidelity depth estimations and Marigold as high quality depth estimation.



Figure 8: Live reconstruction of a leg and coffee table with MiDAS

of MiDaS reconstructions, and the 3rd and 5th row corresponding to the results of Marigold reconstruction. Figure 8 shows the result of reconstruction of a pair of legs and a coffee table with the MiDAS model. Unfortunately, offloading data from the open-source app was incredibly buggy therefore the quality of the image is a little low.

From a visual perspective, the main shortcoming I saw with this approach was that the inferred distance from the image plane to the facial features was largely inconsistent. For example, the subject in the 2nd and 4th column of Figure 7 are roughly equidistant from the camera. Yet the corresponding reconstructions of these faces are incredibly varied. The 2nd subject has a significantly

flatter reconstruction around the cheeks that's not existent in the reconstruction of the 4th subject. Simultaneously we can see that both reconstruction models seemed to have estimated the depth incorrectly for subject in columns 9 and 10. Specifically, the depth model predicted the front cowlicks to extrude outwards which results in a mohawk. From a technical perspective, this makes sense because both MiDaS and Marigold were not trained on a metric accurate datasets. Due to the diversity in the source of the ground truth, all depth values were normalized between 0 to 1, effectively prompting the models to predict relative depth instead of metric accurate depth.

The overall fidelity of reconstructions is not the greatest, and sometimes it's difficult to ascertain whose face is being reconstructed. Increasing the quality of the reconstruction models removes noise by a bit, but sacrifices FPS. We need a way to collect metric accurate sensor data before using our transformation pipeline to project the data. Due to the scope of the project, I wasn't able to allocate enough time + resources to further finetune and quantize the depth estimation models which would have likely helped with increasing the FPS.

4.2 Attempt 2: LiDAR + TrueDepth

Reading the fused LiDAR + TrueDepth data, passing it through the custom upscaled model, and performing the transformations averaged about ~50 frames per second. The main reason behind the throughput being tripled with this approach, was that the majority of the data collection was being done with live sensors instead of any of kind of large-scale neural network inference. I also leveraged the Metal shaders which offloaded a bulk of the parallel computation to



Figure 9: Lidar + TrueDepth reconstruction from iPhone 14 Pro

the GPU. The unified memory architecture allowed to me perform zero-copy computations which dramatically reduced non-compute latency. The upscaler ML model was run via CoreML so most of the computation was offloaded to the Apple Neural Engine; a forward inference was almost instantaneous.

Figure 9 shows screenshots of the live reconstruction through the custom Swift app. In general, the fidelity of the reconstructions is insanely high. It is quite clear that my face is being reconstructed in Figure 9. From the naked eye, the proportions for the reconstructions also appear to be metric accurate. Even though the upscaler model was finetuned with mostly facial images, it still performs well in reconstructing other subjects like a couch or a cat.

The main shortcoming of this approach, however, was the inability to render any occluded pixels. Naturally, the easiest technical solution to this would be to increase the number of LiDAR and camera sensors to fuse data from multiple viewpoints. However, due to the self-imposed engineering constraint of using one device, simply increasing the number of imaging sensors feels a little bit like cheating.

4.3 Attempt 3: Template Modeling

As an FYI, due to some issues while deploying the CoreML model, this attempt wasn't incredibly reliable as even loading the model would completely crash the iPhone. I had to run these tests on my Nvidia Jetson (8 CPU cores, 32 GB memory, Ampere Nvidia GPU)

[19] in order to create visualizations for this report, but was still unable to generate GIFs.

I used saved frames of depth and image data to create the facial reconstructions. Figure 10 visualizes reconstruction via MICA which shows how the facial landmark detection and LiDAR depth estimation come together to render the mesh structure. The figure shows occluded edges through red dots which is important to estimating the face shape for the occluded sections of the images. The corresponding occluded structures on the images are clearly shown in the reconstructions in Figure 11.

The fidelity of these reconstructions is pretty high as shown in Figure 11. The facial features are rendered proportionately; although, I noticed that the MICA more or less ignored rendering the hair. This could be easily solved by fine-tuning MICA with high-fidelity LiDAR scans to measure the depth of individual hair strands. The back of the head is no longer hollow since the model use a texture model as a baseline to extrapolate off of.

I believe that the technical failure of this attempt was more indicative of the limitations of the hardware and software stack rather than the underlying approach itself. Maybe with a bit more of software maturity and/or retooling of the model architecture, I would be able to get more promising results with this hybrid approach over the pure LiDAR-based reconstruction.

5 FURTHER STUDY

Upon achieving decent reconstructions from Attempt 2 with the LiDAR + TrueDepth sensor fusion, it would be interesting to explore basic hardware implementations of projecting holograms into the real-world. Existing research with novel approaches exist [48] [52] [55] [54] [2], however the ultimate goal should be use a novel approach for multi-dimensional light projection.

ACKNOWLEDGMENTS

Special thanks to Aleyosha, Lisa, and Suzie for helping provide the groundwork for this project.

REFERENCES

- [1] Jens Ahremark and Simon Bazso. 2022. Benchmarking a machine learning model in the transformation from PyTorch to CoreML.
- [2] Author8 Author7 and Author9. 2019. Real-time dynamic holographic display using phase-only spatial light modulator. In *Proceedings of the SPIE Photonics West*, Vol. 10944. 109440D.
- [3] Paul J Besl and Neil D McKay. 1992. A method for registration of 3-D shapes. In *IEEE Transactions on Pattern Analysis and Machine Intelligence*, Vol. 14. IEEE, 239–256.
- [4] Stan Birchfield and Carlo Tomasi. 1999. Depth discontinuities by pixel-to-pixel stereo. *International Journal of Computer Vision* 35 (1999), 269–293.
- [5] Reiner Birkel, Diana Wofk, and Matthias Müller. 2023. Midas v3. 1—a model zoo for robust monocular relative depth estimation. *arXiv preprint arXiv:2307.14460* (2023).
- [6] Chen Cao, Yanlin Weng, Shun Zhou, Yiyang Tong, and Kun Zhou. 2013. Facewarehouse: A 3d facial expression database for visual computing. *IEEE Transactions on Visualization and Computer Graphics* 20, 3 (2013), 413–425.
- [7] Xiaotian Chen, Xuejin Chen, and Zheng-Jun Zha. 2019. Structure-Aware Residual Pyramid Depth Estimation. In *Proceedings of the Thirty-Third AAAI Conference on Artificial Intelligence*.
- [8] Xiaotian Chen, Junchen Zhou, Xuejin Chen, and Zheng-Jun Zha. 2022. MonoDepthFormers: Transformers for Computationally Efficient Monocular Depth Estimation. *arXiv preprint arXiv:2209.07688* (2022).
- [9] Angela Dai, Matthias Nießner, Michael Zollhöfer, Shahram Izadi, and Christian Theobalt. 2017. Bundlefusion: Real-time globally consistent 3d reconstruction using on-the-fly surface reintegration. *ACM Transactions on Graphics (ToG)* 36, 4 (2017), 1.

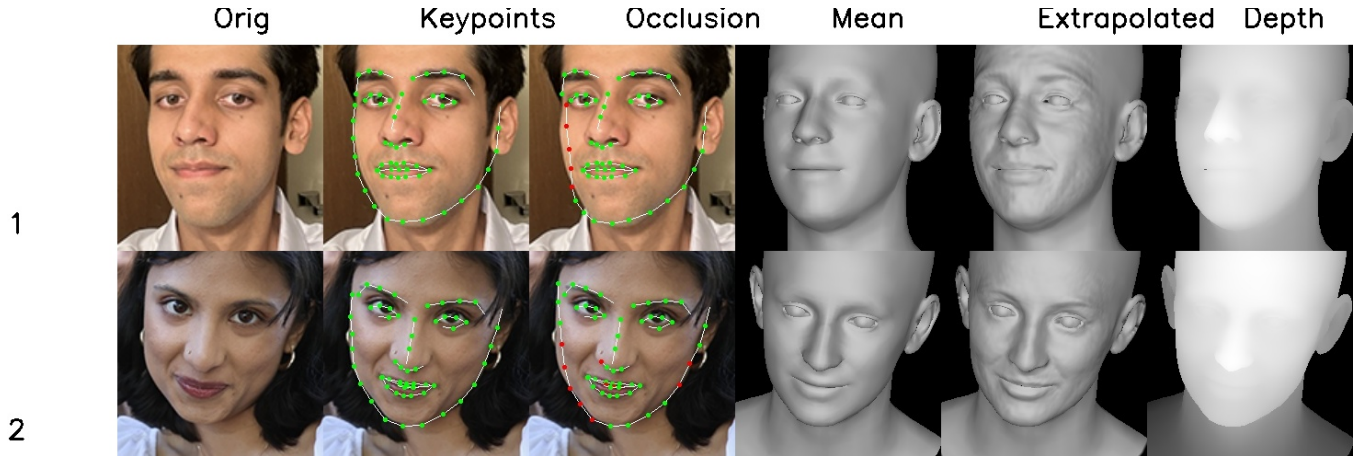


Figure 10: Fused depth + facial landmarks predictions generated by MICA to render 3D mesh of reconstructed face

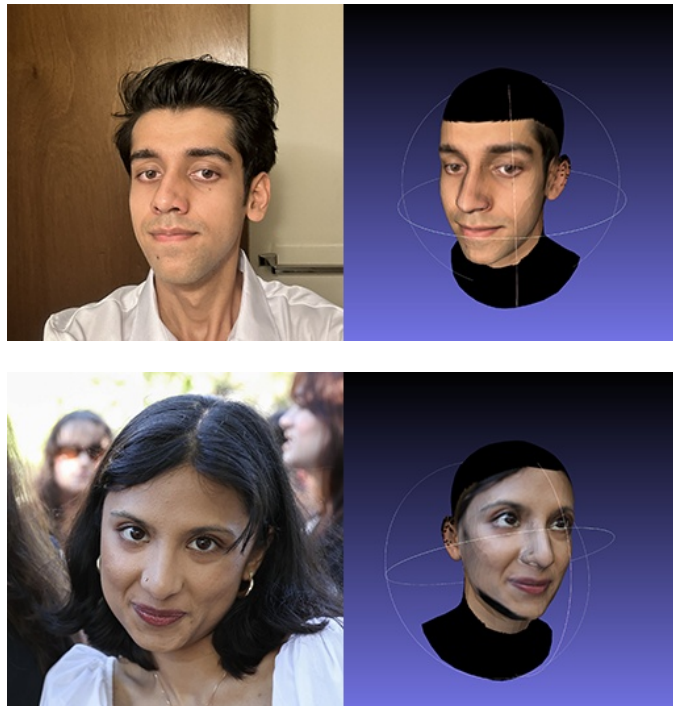


Figure 11: INSTA end-to-end reconstruction with mesh and texture generated given an image of a face (I can already hear Aleyosha’s voice in my head saying "texture is everything" but regardless the reconstructions look incredibly realistic)

[10] Chao Dong, Chen Change Loy, Kaiming He, and Xiaoou Tang. 2015. Image super-resolution using deep convolutional networks. *IEEE transactions on pattern analysis and machine intelligence* 38, 2 (2015), 295–307.

[11] David Eigen, Christian Puhrsch, and Rob Fergus. 2014. Depth map prediction from a single image using a multi-scale deep network. In *Advances in Neural Information Processing Systems*. 2366–2374.

[12] Stephan J Garbin, Davide Schoenmakers, Matteo Leonetti, Rem Hofstede, Thomas Weyrich, and Hans-Peter Seidel. 2021. Efficient neural radiance fields. In *arXiv preprint arXiv:2111.07931*.

[13] Jungong Han, Ling Shao, Dong Xu, and Jamie Shotton. 2013. Enhanced computer vision with microsoft kinect sensor: A review. *IEEE transactions on cybernetics* 43, 5 (2013), 1318–1334.

[14] Peter Hedman, Pratul P Srinivasan, Ben Mildenhall, Jonathan T Barron, and Paul Debevec. 2021. SneRG: Synthesizing normals to render geometry with learned differentiable intersection. In *Proceedings of the IEEE/CVF Conference on Computer Vision and Pattern Recognition*. 8506–8516.

[15] Junjie Hu, Muhammed Ozkan, Yu Seiken, Andrew Zisserman, and Marc Pollefeys. 2019. Revisiting single image depth estimation: Toward higher resolution maps with semi-supervised learning. In *2019 IEEE Winter Conference on Applications of Computer Vision (WACV)*. IEEE, 1949–1958.

[16] Qiangui Huang, Weiyue Wang, and Ulrich Neumann. 2018. Recurrent slice networks for 3d segmentation of point clouds. In *Proceedings of the IEEE Conference on Computer Vision and Pattern Recognition*. 2626–2635.

[17] Shahram Izadi, David Kim, Otmar Hilliges, David Molyneaux, Richard Newcombe, Pushmeet Kohli, Jamie Shotton, Steve Hodges, Dustin Freeman, Andrew Davison, et al. 2011. Kinectfusion: real-time 3d reconstruction and interaction using a moving depth camera. In *Proceedings of the 24th annual ACM symposium on User interface software and technology*. 559–568.

[18] Ren Jiang, Guannan Luo, Wenyuan Liu, Ngan Kwok, and Qizhi Zhou. 2022. LiDAR Point Cloud Reconstruction and Completion via RGB-Guided Voxel Transformers. In *Proceedings of the IEEE/CVF Conference on Computer Vision and Pattern Recognition*. 8766–8775.

[19] Leela S Karumbunathan. 2022. NVIDIA Jetson AGX Orin Series.

[20] Michael Kazhdan, Matthew Bolitho, and Hugues Hoppe. 2006. Poisson surface reconstruction. In *Proceedings of the Fourth Eurographics Symposium on Geometry Processing*, Vol. 7.

[21] Bingxin Ke, Anton Obukhov, Shengyu Huang, Nando Metzger, Rodrigo Caye Daudt, and Konrad Schindler. 2023. Repurposing diffusion-based image generators for monocular depth estimation. *arXiv preprint arXiv:2312.02145* (2023).

[22] Alex Kendall, David B Grimes, and Roberto Cipolla. 2017. GC-Net: Geometric correspondence network for disparity estimation. *The British Machine Vision Conference (BMVC)* (2017).

[23] Mikko Kytö, Mikko Nuutinen, and Pirkko Oittinen. 2011. Method for measuring stereo camera depth accuracy based on stereoscopic vision. In *Three-dimensional imaging, interaction, and measurement*, Vol. 7864. SPIE, 168–176.

[24] Iro Laina, Christian Rupprecht, Vasileios Belagiannis, Federico Tombari, and Nassir Navab. 2016. Deeper depth prediction with fully convolutional residual networks. In *2016 Fourth International Conference on 3D Vision (3DV)*. IEEE, 239–248.

[25] Zhengqi Li, Simon Niklaus, Noah Snavely, and Oliver Wang. 2021. Neural 3D video synthesis from a single semantic image. In *arXiv preprint arXiv:2103.07953*.

[26] Fayao Liu, Chunhua Shen, Guosheng Lin, and Ian Reid. 2015. Learning depth from single monocular images using deep convolutional neural fields. In *IEEE Transactions on Pattern Analysis and Machine Intelligence*, Vol. 38. IEEE, 2024–2039.

[27] Lingjie Liu, Jiatao Gu, Kyaw Zaw Lin, Tat-Seng Chua, and Christian Theobalt. 2020. Neural sparse voxel fields. In *Advances in Neural Information Processing Systems*, Vol. 33. 15651–15663.

[28] Hugh Christopher Longuet-Higgins. 1981. A computer algorithm for reconstructing a scene from two projections. *Nature* 293, 5828 (1981), 133–135.

- [29] Michael Lucente. 1994. Holographic optical elements for optical data processing. *Optical Engineering* 33, 9 (1994), 2768–2779.
- [30] Michael Lucente. 1995. Optimization of hologram computation for real-time photorealistic augmented reality. In *Practical Holography XI*, Vol. 2652. International Society for Optics and Photonics, 309–314.
- [31] Gregor Luetzenburg, Aart Kroon, and Anders A Bjørk. 2021. Evaluation of the Apple iPhone 12 Pro LiDAR for an application in geosciences. *Scientific reports* 11, 1 (2021), 1–9.
- [32] Siheng Ma, Yonghua Bao, Xuanchen Gao, and Dong Cao. 2022. LiDAR-Guided Autonomous Vehicle Trajectory Prediction. In *Proceedings of the IEEE/CVF Winter Conference on Applications of Computer Vision*. 1375–1384.
- [33] David Marr and Tomaso Poggio. 1976. Cooperative computation of stereo disparity. *Science* 194, 4262 (1976), 283–287.
- [34] Ben Mildenhall, Pratul P Srinivasan, Matthew Tancik, Jonathan T Barron, Ravi Ramamoorthi, and Ren Ng. 2020. NeRF: Representing Scenes as Neural Radiance Fields for View Synthesis. In *European Conference on Computer Vision (ECCV)*. Springer.
- [35] Thomas Müller, Alex Evans, Christoph Schied, and Alexander Keller. 2022. Instant neural graphics primitives with a multiresolution hash encoding. In *ACM Transactions on Graphics (TOG)*, Vol. 41. ACM, 1–15.
- [36] Matthias Nießner, Michael Zollhöfer, Shahram Izadi, and Marc Stamminger. 2013. Real-time 3D reconstruction at scale using voxel hashing. *ACM Transactions on Graphics (ToG)* 32, 6 (2013), 1–11.
- [37] Stefan Oehler, Martin Janecic, Ingo Wald, Wolfgang Worner, and Alfredo Delgado-Guzarahah. 2011. Efficient Parallel Hierarchical Radiosity on a Cluster. In *Proceedings of the ACM SIGGRAPH Symposium on High Performance Graphics*. 143–152.
- [38] Cengiz Oztireli, Gael Guennebaud, and Markus Gross. 2009. A computational model of fresco for 3D reconstruction. In *ACM Transactions on Graphics (TOG)*, Vol. 28. ACM, 1–9.
- [39] Quannan Pan, Gerhard Reitmayr, and Tom Drummond. 2013. Probuilding: A robust and memory-efficient voxel reconstruction engine for 3d-scanning systems. In *Computer Graphics Forum*, Vol. 32. Wiley Online Library, 137–147.
- [40] Nick Pears and Christian Duncan. 2016. Automatic 3D modelling of craniofacial form. [arXiv:1601.05593 \[cs.CV\]](https://arxiv.org/abs/1601.05593)
- [41] Yifan Peng, Seung-Hwan Choi, Andrzej Czyzewski, and Aydogan Ozcan. 2020. Deep learning for computer-generated holography. *Advanced Photonics* 2, 4 (2020), 046005.
- [42] Marc Pollefeys, David Nistér, Jan-Michael Frahm, Afshin Akbarzadeh, Philippos Mordohai, Brian Clipp, Christopher Engels, David Gallup, Suk Jin Kim, Paul Merrell, et al. 2008. Detailed real-time urban 3D reconstruction from video. *International Journal of Computer Vision* 78, 2 (2008), 142–167.
- [43] Victor Adrian Prisacariu, Olaf Kähler, Stuart Golodetz, Michael Sapienza, Tommaso Cavallari, Philip HS Torr, and David W Murray. 2017. Infinitam v3: A framework for large-scale 3d reconstruction with loop closure. *arXiv preprint arXiv:1708.00783* (2017).
- [44] Albert Pumarola, Enric Corona, Gerard Pons-Moll, and Francesc Moreno-Noguer. 2021. D-nerf: Neural radiance fields for dynamic scenes. In *Proceedings of the IEEE/CVF Conference on Computer Vision and Pattern Recognition*. 10318–10327.
- [45] René Ranftl, Alexey Bochkovskiy, and Vladlen Koltun. 2021. Vision transformers for dense prediction. In *Proceedings of the IEEE/CVF International Conference on Computer Vision*. 12179–12193.
- [46] René Ranftl, Katrin Lasinger, David Hafner, Konrad Schindler, and Vladlen Koltun. 2020. Towards robust monocular depth estimation: Mixing datasets for zero-shot cross-dataset transfer. *IEEE transactions on pattern analysis and machine intelligence* 44, 3 (2020), 1623–1637.
- [47] Denis Rebain, Wei Jiang, Sorooosh Yazdanpanah, Oussama Ammar, Mathieu Johannink, Baohua Sun, and Bernt Schiele. 2022. DERF: Deformable Neural Radiance Fields. *arXiv preprint arXiv:2208.00885* (2022).
- [48] Alf Ritter, Joachim Böttger, Oliver Deussen, Matthias König, and Thomas Strothotte. 1999. Hardware-based rendering of full-parallax synthetic holograms. *Applied Optics* 38, 8 (1999), 1364–1369.
- [49] Saurabh Saxena, Abhishek Kar, Mohammad Norouzi, and David J Fleet. 2023. Monocular depth estimation using diffusion models. *arXiv preprint arXiv:2302.14816* (2023).
- [50] Daniel Scharstein and Richard Szeliski. 2003. High-accuracy stereo depth maps using structured light. In *2003 IEEE Computer Society Conference on Computer Vision and Pattern Recognition, 2003. Proceedings.*, Vol. 1. IEEE, 1–1.
- [51] Raluca Seona, Mariano Jaimez, Yvan R Petillot, Maurice Fallon, and Daniel Cremers. 2018. Staticfusion: Background reconstruction for dense rgb-d slam in dynamic environments. In *2018 IEEE international conference on robotics and automation (ICRA)*. IEEE, 3849–3856.
- [52] Young-Ho Seo, Hyun-Jun Choi, Ji-Sang Yoo, and Dong-Wook Kim. 2011. Cell-based hardware architecture for full-parallel generation algorithm of digital holograms. *Optics Express* 19, 9 (2011), 8750–8761.
- [53] Liming Shi, Songjiang Ye, Chao Zuo, Ravi S Jonnal, and Laura Waller. 2021. Towards real-time photorealistic 3D holography with deep generative networks. *Nature* 591, 7849 (2021), 258–262.
- [54] Tomoyoshi Shimobaba, Sinsuke Hishinuma, and Tomoyoshi Ito. 2002. Special-purpose computer for holography HORN-4 with recurrence algorithm. *Computer physics communications* 148, 2 (2002), 160–170.
- [55] Tomoyoshi Shimobaba, Nobuyuki Masuda, Takashige Sugie, Satoru Hosono, Shinobu Tsukui, and Tomoyoshi Ito. 2000. Special-purpose computer for holography HORN-3 with PLD technology. *Computer physics communications* 130, 1-2 (2000), 75–82.
- [56] Vincent Sitzmann, Julien NP Martel, Alexander W Bergman, David B Lindell, and Gordon Wetzstein. 2020. Implicit neural representations with periodic activation functions. In *Advances in Neural Information Processing Systems*, Vol. 33. 7145–7156.
- [57] Pratul P Srinivasan, Ben Mildenhall, Matthew Tancik, Jonathan T Barron, Richard Tucker, and Noah Snavely. 2021. Nerv: Neural reflectance and visibility fields for relighting and view synthesis. In *Proceedings of the IEEE/CVF Conference on Computer Vision and Pattern Recognition*. 7495–7504.
- [58] Matthew Tancik, Armen Sadat, Ben Hershey, Charlie Donow, Ben Mildenhall, Ben Fridovich-Keil, and Jonathan T Barron. 2022. Barf: Bundle-adjusting neural radiance fields. *arXiv preprint arXiv:2205.11975* (2022).
- [59] Carlo Tomasi and Takeo Kanade. 1992. Shape and motion from image streams under orthography: a factorization method. *International Journal of Computer Vision* 9, 2 (1992), 137–154.
- [60] Alex Trevithick and Bo Yang. 2021. GRF: Learning a general radiance field for 3D scene representation and rendering. In *arXiv preprint arXiv:2010.04595*.
- [61] Benjamin Ummenhofer, Huizhong Zhou, Jonas Uhrig, Niloy Mujica-Parodi, Tammy Berman, Andrew Duryea, Laurent Kneip, Laura Leal-Taixé, Alina Kirillov, Qiuren Tang, et al. 2017. DeMoN: Depth and motion network for learning monocular stereo. In *Proceedings of the IEEE Conference on Computer Vision and Pattern Recognition*. 5038–5047.
- [62] Zhongqin Wang, Yatong Zhou, Haiyan Zhai, Zhang Lin, Leyuan Wu, Haihan Zhang, Jian Cheng, You Zhou, and Yujun Wang. 2020. DFNet: Exploiting depth-wise separable convolutions for monocular depth estimation. In *IEEE Transactions on Image Processing*, Vol. 30. IEEE, 4886–4898.
- [63] Thomas Whelan, Stefan Leutenegger, Renato F Salas-Moreno, Ben Glocker, and Andrew J Davison. 2015. ElasticFusion: Dense SLAM without a pose graph.. In *Robotics: science and systems*, Vol. 11. Rome, Italy, 3.
- [64] Fan Yang, Guoxuan Li, Xin Zhou, Yuli Wong, and Yifan Zhou. 2018. Towards complete 3d scene reconstruction from egocentric RGB-D semantic mapping. In *2018 IEEE International Conference on Robotics and Automation (ICRA)*. IEEE, 3556–3563.
- [65] Jialong Yang, Hongdong Li, Dylan Campbell, and Yunde Jia. 2016. Go-ICP: A globally optimal solution to 3D ICP point-set registration. In *IEEE Transactions on Pattern Analysis and Machine Intelligence*, Vol. 38. IEEE, 2241–2254.
- [66] Alex Yu, Vickie Ye, Matthew Tancik, and Angjoo Kanazawa. 2021. Pixelnerf: Neural radiance fields from one or few images. In *Proceedings of the IEEE/CVF Conference on Computer Vision and Pattern Recognition*. 4578–4587.
- [67] Stefan Zander, Chris Chiu, and Gerhard Sageder. 2012. A computational model for the integration of linked data in mobile augmented reality applications. In *Proceedings of the 8th International Conference on Semantic Systems*. 133–140.
- [68] Jure Zbontar and Yann LeCun. 2016. Stereo matching by training a convolutional neural network to compare image patches. *The journal of machine learning research* 17, 1 (2016), 2287–2318.
- [69] Pengcheng Zhao, Qingwu Hu, Shaohua Wang, Mingyao Ai, and Qingzhou Mao. 2018. Panoramic image and three-axis laser scanner integrated approach for indoor 3D mapping. *Remote Sensing* 10, 8 (2018), 1269.
- [70] Tinghui Zhou, Matthew Brown, Noah Snavely, and David G Lowe. 2017. Unsupervised learning of depth and ego-motion from video. In *Proceedings of the IEEE Conference on Computer Vision and Pattern Recognition*. 1851–1858.
- [71] Wojciech Zielonka, Timo Bolkart, and Justus Thies. 2022. Instant Volumetric Head Avatars. *2023 IEEE/CVF Conference on Computer Vision and Pattern Recognition (CVPR)* (2022), 4574–4584. <https://api.semanticscholar.org/CorpusID:253761096>
- [72] Wojciech Zielonka, Timo Bolkart, and Justus Thies. 2022. Towards Metrical Reconstruction of Human Faces. In *European Conference on Computer Vision*. <https://api.semanticscholar.org/CorpusID:248177832>